Bulletin de l'Institut Scientifique, Rabat, Section Sciences de la Terre, 2024, n° 46, 55–67 **e-ISSN : 2458-7184**

Geology and metal anomalies of the Kampti-Loropeni greenstone, Burkina Faso (West African Craton)

Géologie et anomalies métalliques des roches vertes de Kampti-Loropeni, Burkina Faso (Craton ouest-africain)

Mathieu Nanema[1], Hermann Ilboudo[2*], Justin Winhyel Some[2], Ignace Dabone[3]

1. *Technologies et Géosciences Consult (TEGECO), 18 BP 230 Ouagadougou 18. nanemageologue@gmail.com.*
2. *Université Joseph KI-ZERBO. UFR/SVT. Département des Sciences de la Terre, Laboratoire Géosciences et Environnement, 03 BP 7021 Ouagadougou 03, Burkina Faso.*[*]*(hermann.ilboudo@ujkz.bf).*
3. *Bureau des Mines et de la Géologie du Burkina (BUMIGEB), 01 BP 601 Ouagadougou 01, Burkina Faso.*

Abstract. Stream sediment geochemistry is a method of regional exploration to screen wide areas, of difficult access or high rainfall marked by significant forestry development. This method, combined with remote sensing, petrographic, analytical studies and field work, has enabled us to highlight areas of metal anomalies in the Kampti-Loropeni greenstone in south-west Burkina Faso. The correlation matrix shows multiple mineral associations: (i) the dominance of gold (Au) and gold-molybdenum (Au-Mo) anomalies in the intrabelt basin along the NNE-SSW fault, (ii) the spatial distribution of strategic metals such as lithium-uranium (Li-U), Ta-Nb-Pb-U along with the granite intrusions and (iii) the base and precious metals such as gold-manganese (Au-Mn), copper (Cu), nickel (Ni), zinc (Zn), cobalt (Co) and titanium-vanadium (Ti-V) within the volcanic sequence of Kampti affected by both NNE and NNW-SSE faults. Granite emplacement would have controlled the distribution of strategic metals. Such occurrences like Au-Mn, Cu-Ni-Zn, Co and Ti-V anomalies were hosted both by basaltic rocks and mafic intrusions, strongly deformed and hydrothermalised evidenced by the strong veining system (quartz, carbonate), sulphidation and native metal (Au).From geophysics lineaments and trusted in the ground, NNE-SSW and NNW-SSE fault zones were highlighted overprinting regional NE foliation. Three main geological domains are defined: (i) a broader quartz-feldspar rich volcano-sedimentary domain in contact with (ii) an eastern magmatic domain of mafic composition and (iii) a granitoid pluton intrusive in both domains.

Keywords: Stream sediment, polymetallic occurrences, exploration target, greenstone, Kampti-Loropeni

Résumé. La géochimie des sédiments de ruisseaux est une méthode d'exploration régionale dans les zones difficiles d'accès ou à forte pluviométrie marquées par un développement forestier important. Cette méthode combinée à la télédétection, à l'étude pétrographique et analytique ont permis de mettre en évidence des zones d'anomalies métalliques (indices) dans leur contexte géologique le long du prospect de Kampti-Loropeni au sud-ouest du Burkina Faso. La matrice de corrélation montre de multiples associations métalliques : (i) la dominance des anomalies d'or (Au) et d'or-molybdène (Au-Mo) dans le bassin métasédimentaire le long de la faille NNE-SSW, (ii) la distribution spatiale des métaux stratégiques tels que lithium-uranium (Li-U), Ta-Nb-Pb-U à proximité des intrusions granitiques et (iii) les signaux métalliques d'or-manganèse (Au-Mn), du cuivre (Cu), du nickel (Ni), du zinc (Zn), du cobalt (Co) et du titane-vanadium (Ti-V), dans la série magmatique de Kampti le long de la faille NNW-SSE. La mise en place des granites aurait contrôlé la distribution des métaux stratégiques. Le contrôle lithologique et structural des anomalies Au-Mn, Cu-Ni-Zn, Co et Ti-Vdans des roches(volcanites et intrusions diverses) fortement déformées et hydrothermalisées est,en témoigne les nombreuses émanations de filons (quartz, carbonate), sulfures abondants et métaux natifs (principalement or). La géophysique aéroportée (signal analytique et radiométrique) combinée à des études de terrain ont identifiés des zones de failles NNE-SSW et NNW-SSE surimposant des structures régionales NE et des dykes NW. Trois domaines géologiques principaux sont clairement définis: (i) un domaine volcano-sédimentaire plus large riche en quartz-feldspath en contact avec (ii) un domaine magmatique oriental de composition basique et (iii) un ensemble de corps granitique intrudant les deux domaines.

Mots clés : Sédiments de ruisseaux, indices polymétalliques, cible d'exploration, roches vertes, Kampti-Loropeni

INTRODUCTION

Within the southern West African Craton (Fig. 1), the host to primary metal are associated to Precambrian greenstone rocks (Allibone 2002, Baraou *et al*. 2021, Bonzi 2021, Masurel *et al*. 2021). Those metal occurrences were identified through successive exploration approaches implying geochemistry sampling and drilling particularly within the orogenic belts. One method which appears as an effective and proven approach to large-scale mineral exploration in both forest and regions with high hydrographic network, remains the stream sediments geochemistry. It is particularly usefully to screen quickly at low-cost wide area of interest and enable to appreciate the geological background in areas of poor exposures (Bellehumeur *et al*. 1994, Boulahcen *et al*. 2010). Exploration beneath suppressive soil layer or regolith requires good techniques in the aims at highlighting geochemical features and their relationships with litho-tectonic units, metallogenic provinces, and targeting districts.

In the sWAC, research and published papers devoted to effectiveness of exploration method of stream sediment (Dan *et al*. 2012, Khan *et al*. 2022) are very limited or poorly documented, and existing data can be found in the statutory reports of mining companies. The present article is a challenge devoted to regional sampling of stream sediments and the relationship with geological context in southwest Burkina Faso. It focuses on the southern part of the Houndé belt in the

Kampti-Loropeni districts, which constitutes a magmatic and sedimentary complex, a reservoir of metalliferous substances. Clearly, this work involves combining remote sensing and geology to constrain the geochemical anomalies of the study area. The Houndé metallogenic belt is a magmatic assemblage northerly trending and composed of dominant volcanic rocks, meta-sedimentary basins that are all intruded by felsic rocks; all formations are affected by the Eburnean orogeny (Hein 2015, Augustin *et al*. 2017, Nanema 2021). Kampti-Loropeni are metallogenic subdomains fully integrated on the eastern margin of the belt.

Houndé belt is one of the most prolific for gold and base metal as evidenced by the discovery and the mining of such commodities (Mana gold deposit 2.28Moz @ 1.89g/t, Endeavour 2021; Bagassi gold deposit 1.9 Moz @ 9g/t, Rox Gold 2020; Houndé gold deposit 5.7 Moz @ 1.57g/t, Endeavour 2022 and Kiéré Manganese deposit 1.1 Mt @ 44%Mn, USGS 2011) and several base metal occurrences (Castaing *et al*. 2003). The Bureau des Mines et de la Géologie du Burkina (BUMIGEB) completed a regional stream sediment survey in 2015 in the south-eastern portion of the Houndé belt including the Kampti-Loropeni greenstone. In this study, the results are meaningfully interpreted metal anomalies to enhance mineral exploration. The recent study is a contribution to better define the potential of that portion of the belt with the geology to highlight new occurrences. Metal associations in term of positive or negative correlation were constrained and it could be used as guide for small and large-scale exploration and can be integrated in the metallogenic portfolio of Burkina Faso mineral system.

GEOLOGICAL BACKGROUND

The NNE to NE architecture of the greenstone belts surrounded by the Tonalite-Trondhjemite-Granitoid (TTG) complex in Burkina Faso form part of the global dynamic accretion of a juvenile crust of the Leo/Man shield in the southern West African Craton (sWAC) (Fig. 1). The related Paleoproterozoic formations implying variable lithologies are metamorphosed and deformed; geochemically range from alkaline to tholeiitic affinities (Bessoles 1977, Boher *et al*. 1992). The mafic volcanic segment along the Houndé belt in SW Burkina is identified as Tehini belt in Northern Côte d'Ivoire and expands 200 km long, flanked to west to the high strain zone of the meta-sedimentary rocks and widening towards the south where it borders the highly metamorphic Awaikro basin. In the study area (Fig. 2A), the meta-sedimentary rocks are deposited in the intrabelt basin to the west and the tholeiitic volcanic rocks to the east which forms the Kampti-Loropeni greenstone comprising (i) a dominant basalt flows at the base of the volcanic pile followed by andesitic pyroclastite (Nanema *et al*. 2017). This sequence is crosscut by (ii) stocks of orthôcumulate gabbro, diorite and felsic dykes. The overall is subsequently intruded by granitoid batholiths and bordered to the east by (iii) granitic gneiss. The westward transition to the calc-alkaline segment is mixed with some tholeiitic occurrences that are contemporaneous to their emplacement (Augustin & Gaboury 2016). These two volcanic segments are separated by the intrabelt graben composed of fine to medium-grained strongly metamorphosed sediments and coarse detrital products made up of polymictic conglomerates, quartz sandstones and dominant siltstones. These detrital rocks emplaced in distensive setting from fluvio-deltaic environment, as a result of the neighboring Birimian belts erosion (Bonkougou 1994, Pouclet *et al*. 1996, Ludtke *et al*. 1998) or as late Birimian molasse deposits (Koffi *et al*. 2016). Two major NNE-SSW Boni (Castaing *et al*. 2003, Baratoux *et al*. 2011) and NNW-SSE Kampti shear zones (Nanema 2021) structured the formations. The arcuate landform is the result of polyphase tectonics, with NNE-SSW

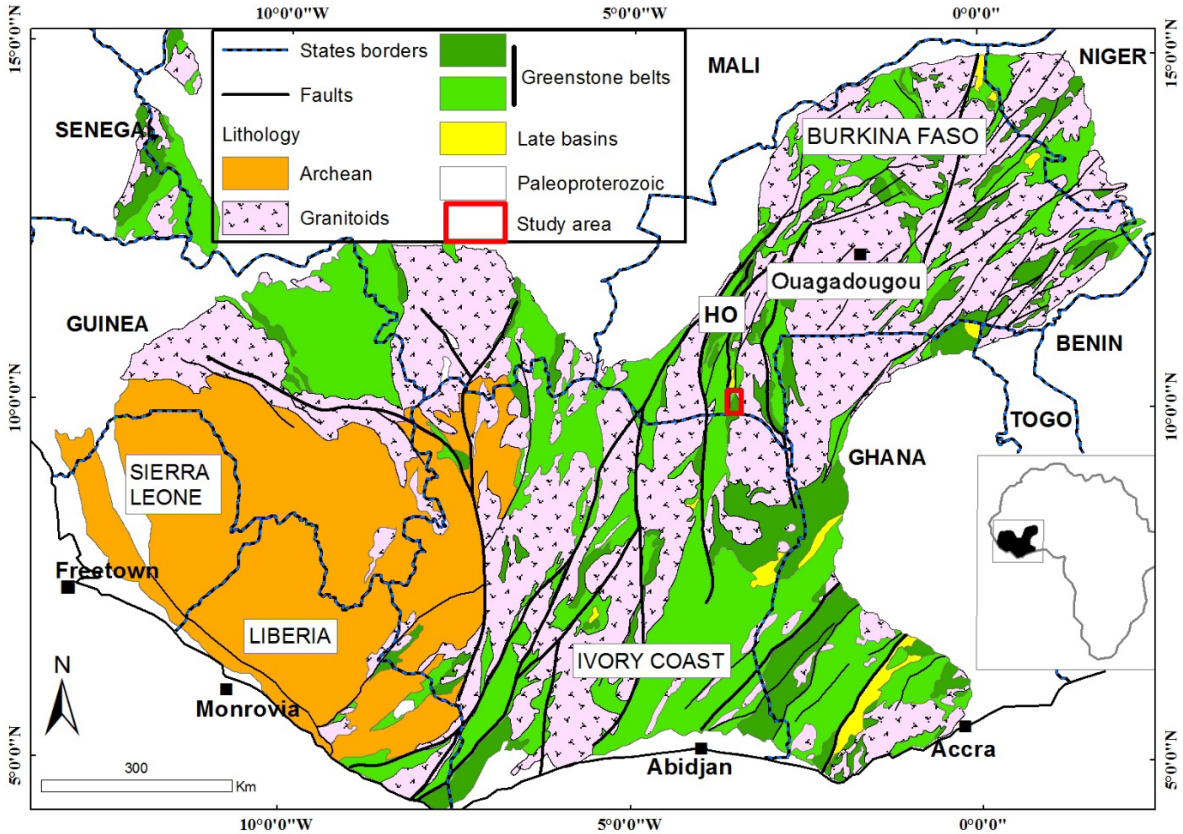

Figure 1:Geological map of the Leo/Man ridge, modified after Block *et al*. 2015.

to NE-SW oriented hill ridges and the main hydrographic network is eastern to submeridian (Fig. 2B).

METHODS

Satellite imagery and Geophysics

The satellite imagery scene 196/53 downloaded from the US Government database (https://www.usgs.gov/) was captured on February 26, 2016. The images were corrected ortho-metrically and geometrically, then georeferenced in WGS84 (UTM30N) with Envy software. The data includes Landsat 8 and DEM were used to extract the drainage flow, access, and the lineaments.The hydrographic network was automatically extracted from the DEM image and ranked. The watersheds are defined and then the BLEG stream sediment sampling sites planed accordingly. The Compagnie Générale de Géophysique (CCG) completed the airborne survey of the metallogenic region of southern Burkina in 1998 as part of the SYSMIN (système minier) project. The flight lines of 500m to 1km spacing and at 100m altitude following a NW-SE trend enable to acquire high resolution data (magnetism and radiometrics) with a Cintrex CS2 cesium fume magnetometer coupled to a high precision GPS. The compiled data obtained from the BUMIGEB were reinterpreted to (i) highlight the main lithological contacts, (ii) the main fracture network and shear zones and (iii) discriminate the lithology that would be integrated for the interpretation of multi-element assay results.

Sampling

The stream sediment sampling was conducted by the BUMIGEB during the wet season from October 2015 to end February 2016. Recent alluvial material was collected on the third order drainage system which allows a minimum area square of anomalism (Fig. 3A). Each sample consists of a composite of at least 5 sampling points in the fine sediment fraction. Samples are taken in the stream bed at intervals of a few dozen meters on either side of the ideal sampling point, which is adjusted from the theoretical point to suit field conditions (Fig. 3B**)**. This ensures that each sample is as representative as possible. The sample is preferably taken using a small shovel made of resistant, non-contaminating plastic. When the collected material is sufficiently dry, it can be pre-sieved on site using a sieve column consisting of a bottom, a 250 µm sieve, a 500 µm sieve and a lid. Only the fraction < 250 µm is retained. A sample of around 2 kg of dry material <250 µm is assumed to be sufficient for dispatchment. It will be placed in a transparent plastic (polyethylene) bag and sent to the laboratory, where it will be further dried if necessary (at 60°C).

If the material is too wet to be sieved on site, the sample is bagged wet without sieving, in the same type of polyethylene plastic bag as above. In this case, the mass to be sampled will be of the order of 5 kg wet. These samples undergo pre-drying at base camp and complete drying in the sun or in an oven not exceeding 60°C. Dried samples are pulverized using a porcelain mortar and sieved using a column of sieves with respective mesh sizes of 500µm and 250µm. The fraction <250**µm is subdivided into four portions using a riffle splitter to obtain 2 bags of** 2000g (+/- 100g) each. One bag is stored as back-up on the BUMIGEB facility (Fig. 3C) and another sent to lab.

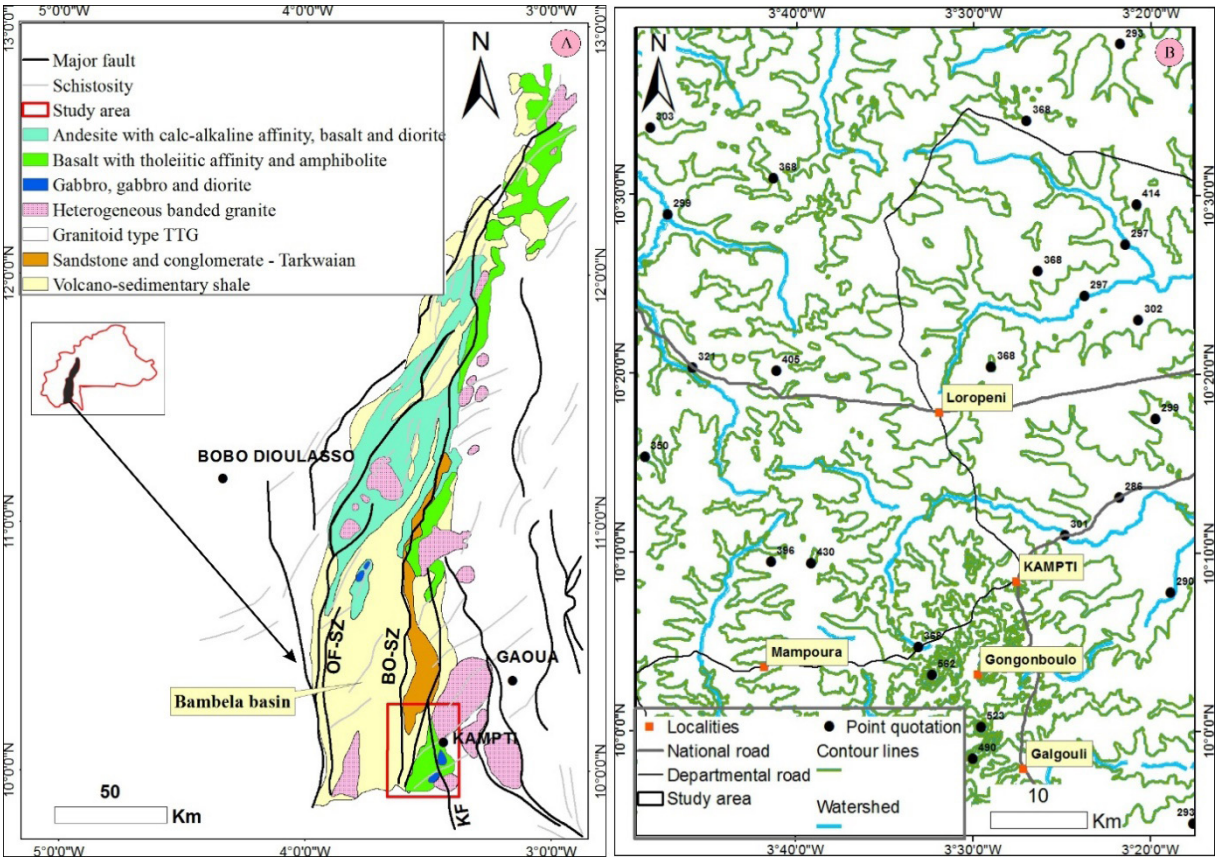

Figure 2:(A) simplified geological map of the Hounde greenstone belt (modified after Nanema 2021). OF-SZ: Ouango-Fitini Shear zone, BO-SZ: Boni Shear zone, KF:Kampti Fault; (B) main drainage system of the Kampti-Loropeni area

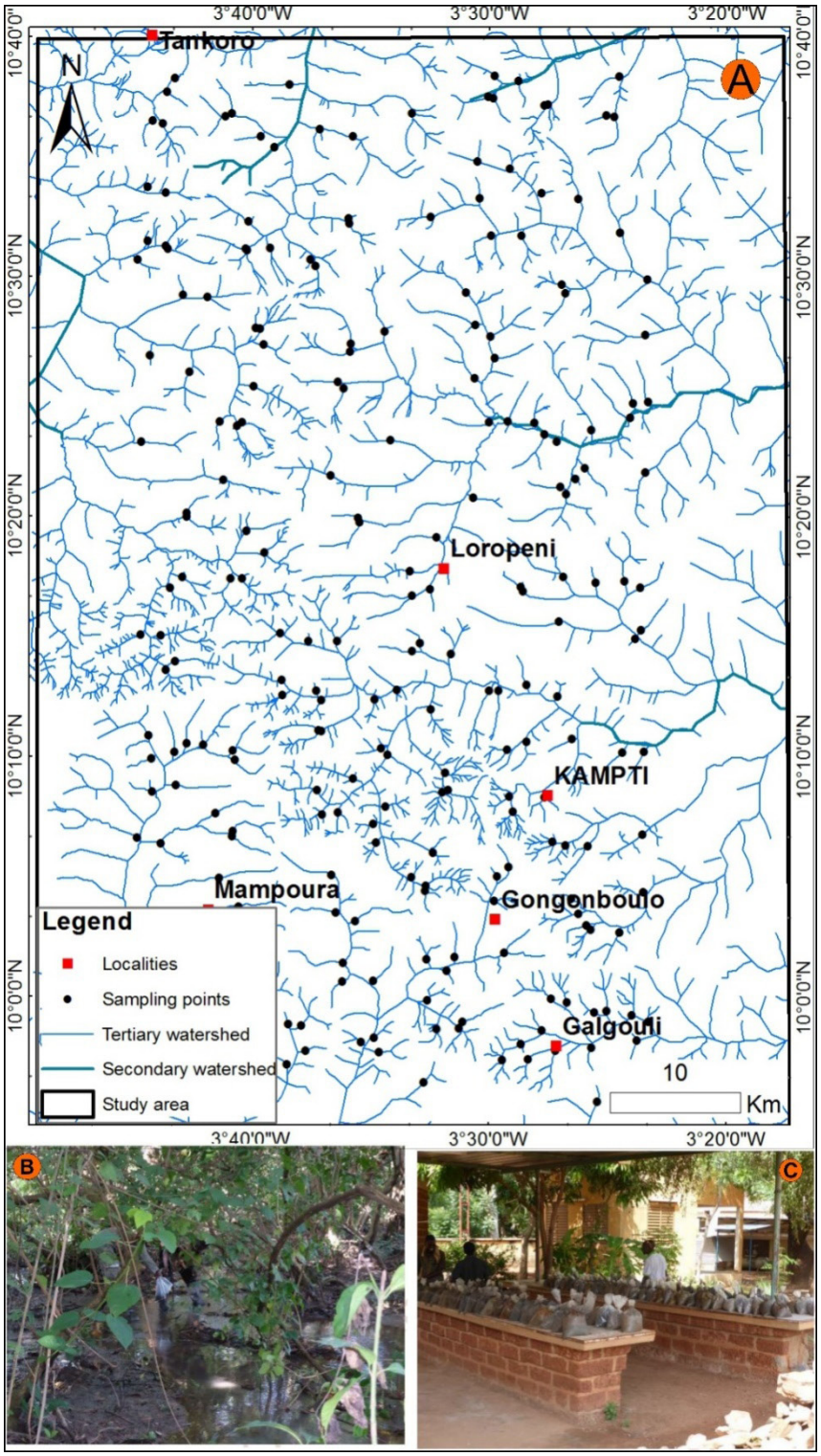

Figure 3:(A) stream sediment sampling points location along the drainage system;(B) rivershed sampling location(C)BUMIGEB lab facility.

Analytical method

The stream sediment samples were analyzed for major, trace and rare earth elements (REE) as well as metals including Au at the ALS-Minerals-Geochemistry laboratory in Loughrea (Ireland). Major elements were assayed by ICP-AES, trace and rare earth elements were by ICP-MS technics after quadri-acid digestion. The four-acid digest can effectively dissolve almost all rock-forming minerals.Major elements are expressed as a percentage by weight (%), as traces and REE in parts per million (ppm) or parts per billion (ppb).

The calculation of the transition element correlation matrix (Au, Mn, Mo, Cu, Ni, Zn, U, Ag, Pb and Co) for 233 samples highlighted mineral associations with positive correlation coefficients above 80%: Au-Mn-Mo; Cu-Ni-Zn; U-Ag-Pb and Co-Mn. The results of these statistical studies are shown in Table 1. Anomaly thresholds for each metal element were defined using the percentile statistical method (Tab. 2).The

quantile or percentile statistical method is used to identify subpopulations with consistent chemical and mineral affinities (Zuo *et al*. 2021). This method can reveal mineralization that may not be discernible from raw assay values and can enhance the geochemical anomalies signal from regional background noises related to lithological and/or environmental origin (Trépanier 2006). However, this method may have limitations in analyzing geochemical data. It can be influenced by the type of mineralization, secondary environment, and sampling grid. In this analysis, it is assumed that values at the 90th percentile (0.9 quantile) in the population are considered anomalous.

Field mapping

The field validation of the geochemical anomalies identify from the 2015/2016 stream sediment campaign were carried out in the year period of 2020-2021. The Geological transects followed along east-west axis perpendicular to the NNE direction of the geological formations. Some orpaillage shafts and explorations trenches were visited and mapped to record the structural fabrics and collected further samples for petrographic studies purpose.The field samples were collected by hammer and referenced using Garmin GPS in the WGS84 geodetic system and UTM North Zone 30 projection.

A dozen thin and polished sections were produced at Joseph Ki-Zerbo University, for microscopic observations.

RESULTS

The remote sensing data

In the study area, a network of lineaments spanning several kilometers is extracted, forming a submeridian corridor (Fig. 4A). On the both side side of this corridor, dispersive discontinuities of lesser extent are oriented NE-SW. Stereographic analysis shows major density poles NNE-SSW and NE-SW and minor trends NNW-SSE; NW-SE; E-W. Reduced to pole Magnetic survey reveals NNE-SSW and NNW-SSE oriented lineaments, confirmed by field observations of mylonitic foliation corridor. These fabrics align with regional ductile/brittle shear corridors. (Fig. 4A). The density contrasts of the U-K-Th spectra (Fig. 4B) impose blue-violet hues bathed and a characteristic dark ochre mass on the southeast corner of the study area, while to the west they are relayed by reddish hues. This analysis distinguishes three main lithological families: (i) mafic units with dark hue signal, (ii) a reddish hue characteristic of felsic to intermediate sediments and (iii) regular-shaped felsic intrusions marked by blue-violet hue (Fig.5).

Table 1: Correlation matrix of 11 of the 49 elements analyzed, out of 233 samples.

	Ag	*As*	*Au*	*Co*	*Cu*	*Mn*	*Mo*	*Ni*	*Pb*	*U*	*Zn*
Ag	1										
As	-0.15947	1									
Au	-0.06369	0.27414	1								
Co	-0.03038	0.28435	0.68758	1							
Cu	0.0476	0.28418	0.25563	0.71377	1						
Mn	-0.10492	0.24849	0.41192	0.82121	0.69111	1					
Mo	0.08565	0.16325	0.40284	0.35712	0.16878	0.1598	1				
Ni	0.07236	0.20068	0.16355	0.6636	0.87755	0.65387	0.1040	1			
Pb	0.35554	-0.22139	-0.16207	-0.36453	-0.40581	-0.42404	0.36963	-0.32824	1		
U	0.35075	-0.31931	-0.11265	-0.36614	-0.51769	-0.42202	0.30189	-0.42585	0.9119	1	
Zn	0.04323	0.22298	0.12175	0.61549	0.90414	0.70574	0.07842	0.87612	-0.33962	-0.46294	1

Table 2: Summary table of calculated percentiles for each metal study.

Percentile	Au (ppb)	Mn (%)	Mo (ppm)	Co (ppm)	Cu (ppm)	Ni (ppm)	Zn (ppm)	Li (ppm)
85%	7	1180	0.79	33.5	60.6	47.3	55	17.6
90%	13	1390	0.89	40	69.5	53.5	65	18.5
95%	27	1790	0.98	50.7	76.4	69.6	79	22
97%	44	1890	1.07	56.7	81.8	86	90	24.1
99%	133	2360	1.73	84.4	113.5	196	103	35

Percentile	U (ppm)	Ag (ppm)	Pb (ppm)	Nb (ppm)	Ta (ppm)	Ti (%)	V (ppm)
85%	3.1	0.06	14.3	24	1.75	0.82	164
90%	3.5	0.06	15.2	25.4	1.84	0.93	177
95%	3.9	0.07	17	27.7	1.99	1.09	221
97%	4.1	0.1	17.3	29	2.22	1.2	256
99%	4.9	0.15	18	31.9	2.81	1.52	302

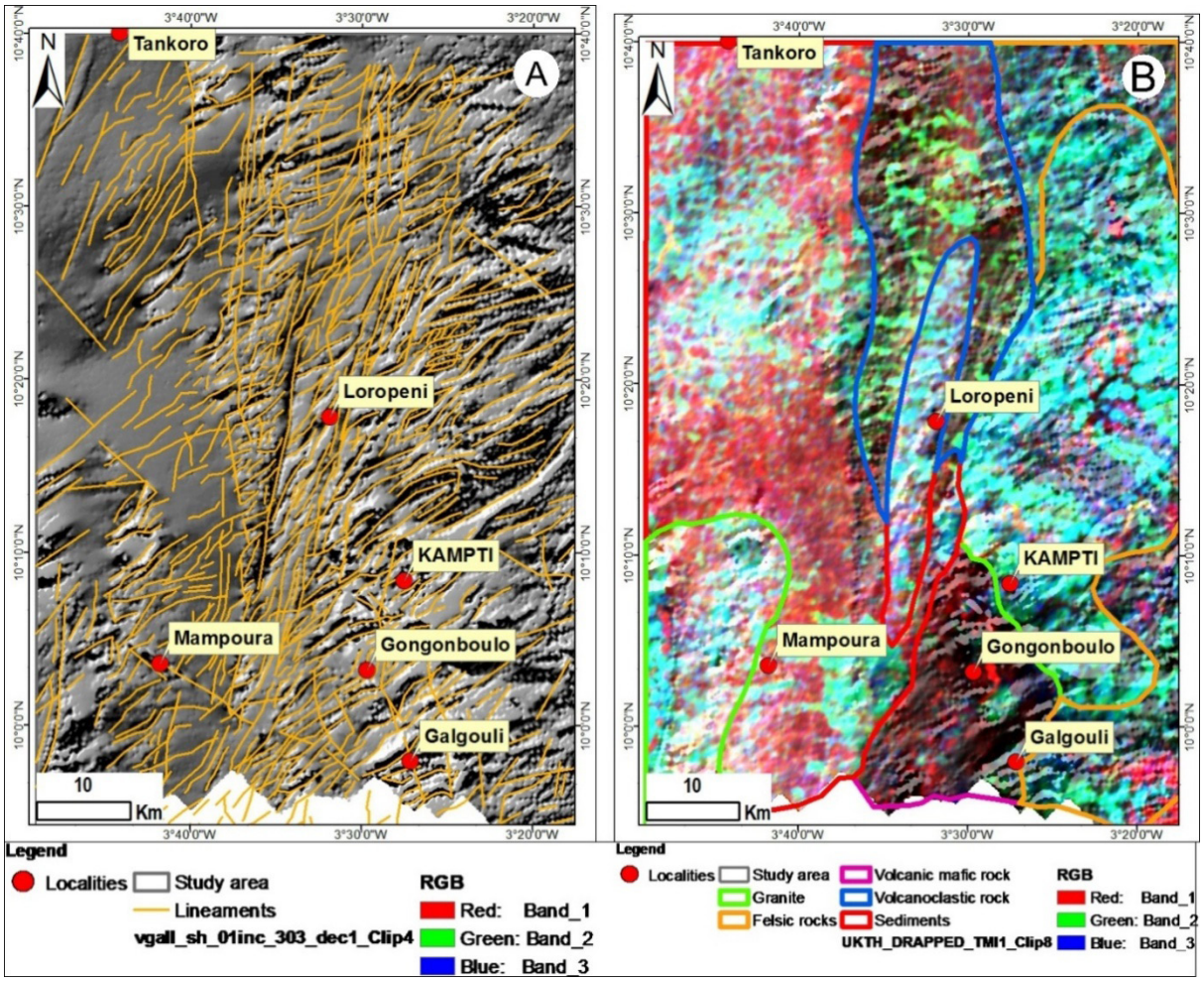

Figure 4: Airborne geophysical imagery of the study area.(A): Total magnetic intensity and interpreted lineaments; (B):Spectral imaging of the radiometry (UKTh) with interpretation of the most important lithological features.

Geology

The study area is dominated by: (i) the Kampti volcano-plutonic sequence on the south corner of the study area; (ii) an intra belt volcano-sediment unit; and (iii) a granitoid unit intruding both sequences (Fig.5). Main lithology composing the entire geology are the followings:

*Meta-basalt flow***.** Basalt flows crop as pseudo-pillow **(**Fig.6a).in the southeastern part of the study area, forming hills along NE direction. Fresh specimens are typically dark green color, generally aphanitic± vesicular. Under microscope, there is a mixture of crystals and granular textures develops by common mineral assemblage such plagioclase, pyroxene, hornblende. The latter is altered into chlorite and epidote (Fig.6b). Calcite, quartz, and opaque minerals are minor phases filling cavities and fractures.

*Meta-pyroclastic rocks***.** The units occur in pseudo-pillow with elongated fragments (Fig.6c) ranging from lapilli to medium grained andesitic crystal tuffs. The matrix contains subangular fragments that have cavities infilled with oxides, chlorite, epidote, and carbonates. The fragments themselves are composed of various lithic elements, including porphyritic andesite with plagioclase ± amphibole, porphyritic microdiorite, minor dacite and rhyolite fragments. Overall fragments are linked by andesitic cement and has a tuffaceous to ashy texture. In addition, it contains mm-sized lithic elements, crystals such as plagioclase and amphibole (occasionally quartz), and frequently has vacuoles filled with minerals like quartz, epidote, calcite, and chlorite (Fig. 6d).

*Meta-gabbro***.** These units crop out in the form of stocks varying between leucocratic gabbro, gabbronorite to melanocratic norite (Fig. 6e) featured by coarse-grained zoned plagioclase, amphibole, and pyroxene. Microscopically, the plagioclases and amphiboles are almost entirely altered. In the deformation corridors, the texture becomes granoblastic, with significant recrystallization of albite and quartz resulting from plagioclase destabilization.

Granitoids. There is a set of heterogranular granite, quartz monzodiorite, trondhjemite and pegmatite. Some of them contains enclaves extracted from nearby country rocks. Generally, they appear leucocratic (Fig.6f), with interstitial quartz, plagioclase, microcline, orthoclase, muscovite, biotite ± amphibole (Fig.6g). The edges of the pluton have undergone intense polyphase hydrothermal alteration implying albite, muscovite, epidote, carbonate, sericite, chlorite and secondary quartz. In addition, we observe some sulphidation and gold-bearing quartz veins.

*Epiclastic formations and derived shales***.** This sequence is the most representative of the intra-belt basin and form continuous northeast bands. The grain size decreases from east to west, progressing towards the basin's center, with a pronounced prevalence of fine facies characterized by tuffaceous origin, with intercalation of minor chemical

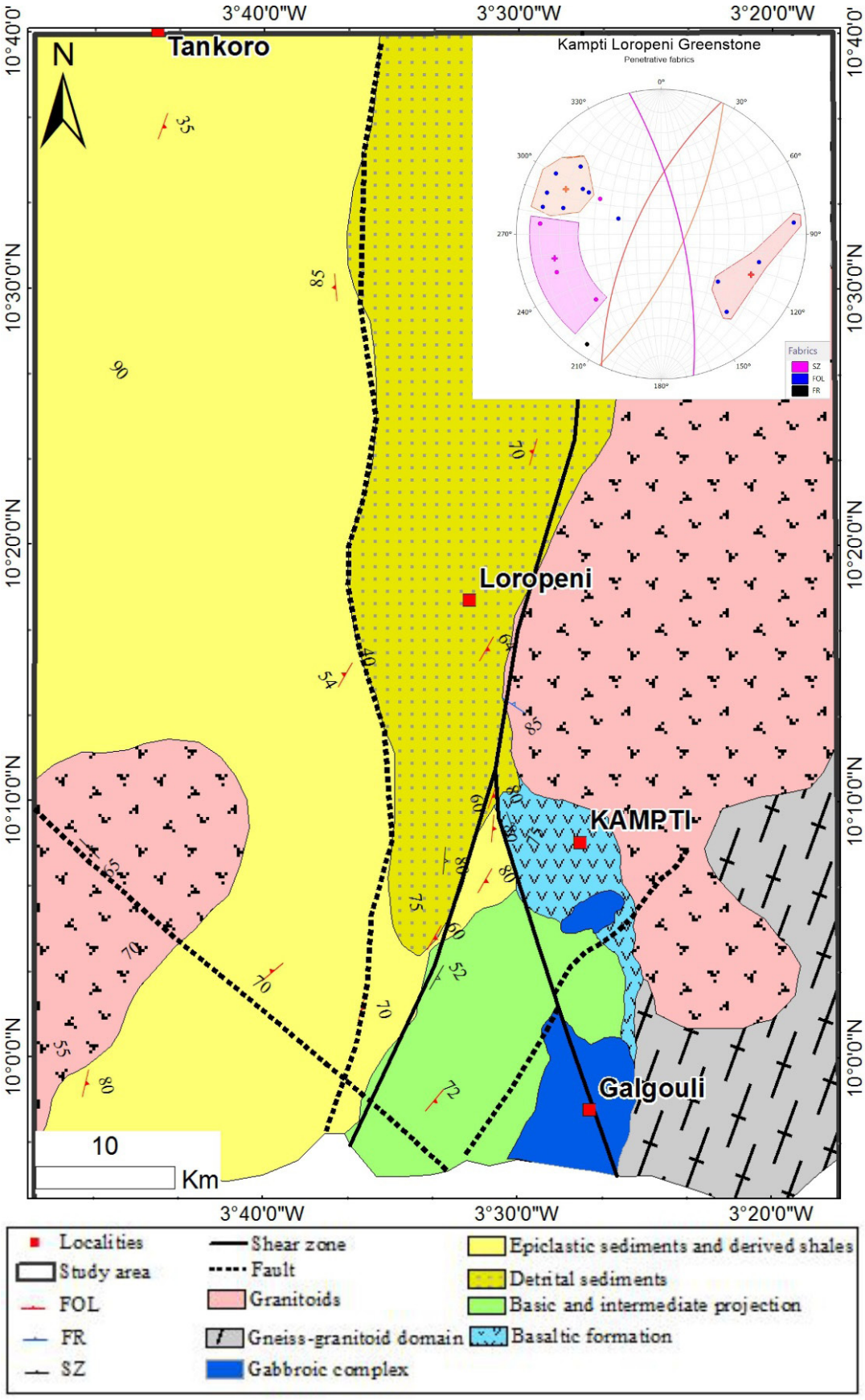

Figure 5: Geological map of the Kampti-Loropeni greenstone.

and detrital sediments. These comprise micaceous schists, quartz-mica schists, graphitic schists, greywackes and similar formations.

*Tarkwa-type detrital formations***.** It forms a sub meridian layer unit, exhibiting near-continuous distribution. Outcrops are poorly exposed in this region, sometimes appearing as band. Primarily comprised of ripple marks on bedding surfaces, cross-bedding arkosic sandstones and conglomerates (Fig.6h). Microscopic examination reveals a ribbon-like arrangement of quartz and quartz-mica layers with poorly sorted grains. Laminae consists predominantly of 70% polycrystalline quartz aggregates, alongside plagioclase, microcline, and felsic lithic pebbles. Alteration of microcline edges to white micas is evident. Sericite, brown biotite, quartz, and plagioclase flakes dominate the cement (Fig.6i). Scattered throughout the matrix are cubic and xenomorphic opaque minerals.

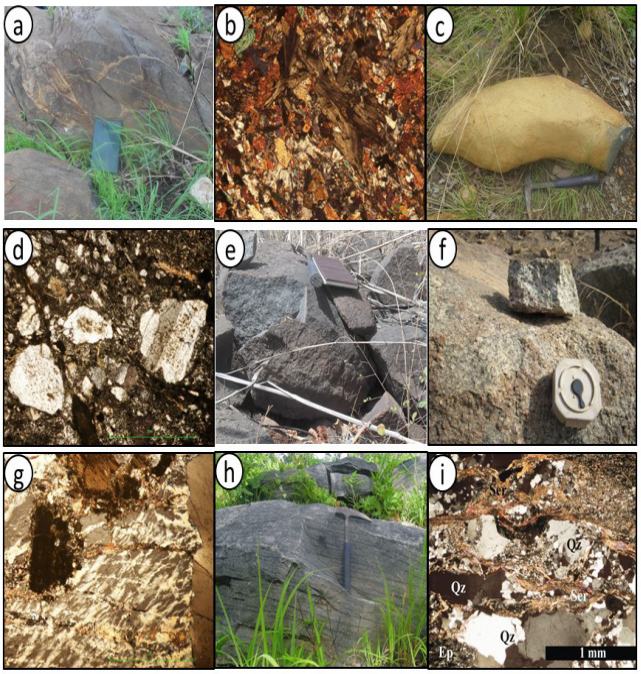

Figure 6**:**(a) outcrop of pillow basalt; (b) microphotograph of basalt; (c) pillowed pyroclastic rock; (d) microphotograph of pyroclastic tuff with brecciated polygenic elements and plagioclase crystals; (e) melanocratic norite; (f) granite; (g) microphotograph of granite; (h), cross-bedded arkose sandstone.; (i) microphotograph of sandstone with of quartz-feldspar and micaceous rich beds.Qz: Quartz; Ep: Epidote; Ser: Sericite.

Deformation and metamorphism

The study area shows evidence of both strong ductile and brittle deformation on the greenstones, with visible structures such as foliation, folds, shear corridors, and vein structures.

The ductile deformation is expressed by the subvertical S1 foliation, which affects all lithologies (Fig.7a), and the associated F1 fold which plunges gently or moderately to the NE (Fig.7b). South of the Loropeni locality, some primary fabrics such as bedding have been preserved in the conglomeratic unit. This stratigraphic unit (N190°/45°) is unconformable with the surrounding schistosed volcanogenic sediments. The mylonitic S2 foliation is overprinted on S1 and is recorded along NNE and NNW deformation corridors. F2 sheath folds are frequently encountered, as are reef and transposed veins. The F2 fold axes recorded in this corridor have varying plunges, ranging from 40° to the north to 70° to the south. The field relationships between the S and C planes suggests a sinistral movement. The mylonitic S2 foliation is also associated with the crenulated schistosity present in these D2 shear zones.The veining system structures consists of quartz -carbonate with a predominant NNE, NE, NNW direction.The first generation of veins (QV1) are aligned parallel to the S1 foliation and folded (Fig.7c).The vein along with the shear corridors NNW and NNE are also auriferous and mineralised in sulphide and suggested to artisanal orpaillage in the Kampti district.

Brittle deformation also affects all lithological units and being most intense during the later phases of deformation. The cleavages and mineral filled fractures (chlorite, calcite, quartz and sulphide) have different orientations. The main network sets are E-W, NW, and ENE. NNW and NNE-trending fractures are observed in the D2 shear zones (Fig.7d).

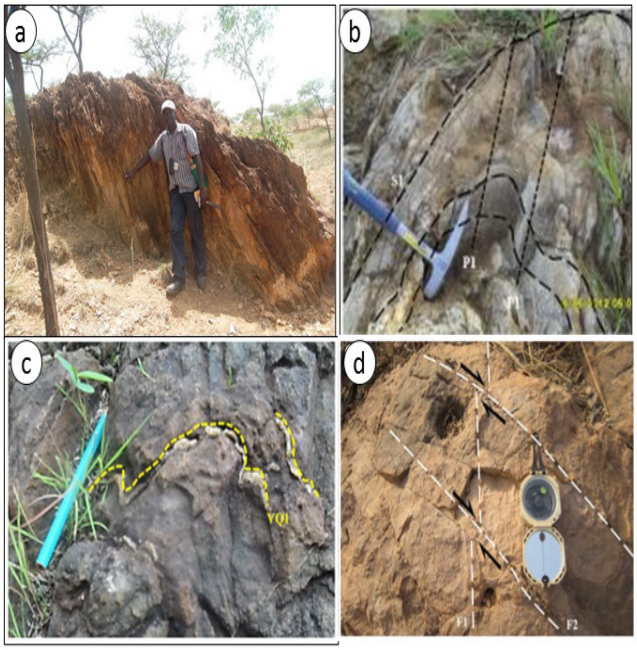

Figure 7: Field photograph of macro structures. (a):mica schist with S1: N025°/70°; (b):isoclinal fold in graphitic shale whose P1 fold axes plunge 25° towards the NE; (c): deformed basalt with early folded extensional quartz veinsVQ1 (N055°/72°) basalt; (d): dextral movement of F1 cleavages (N295°/65°) within pink sandstone.

Three types of metamorphic transformations have been identified in the study area. Regional metamorphism is characterized by mineral assemblages that vary according to the nature of the geological formations. The dominant mineralogical assemblage (ouralite, chlorite, biotite, muscovite, albite, carbonate, epidote, and quartz) suggests low-grade greenschist metamorphism. Contact metamorphism is characterized by actinote - green hornblende - albite or green hornblende - biotite - albite mineral assemblages. Successive phases of deformation are accompanied by hydrothermal fluid circulation. Typical mineral assemblages also depend on the petrographic nature of the host rock. A summary of hydrothermal alteration minerals is given in Table 3.

Metallic signatures from stream sediment geochemistry

The spatial distribution of anomalies

The spatial distribution of metal anomalies is presented in (Fig. 8). Gold (Au) distribution shows two anomalous zones the largest of which is located to the southeast of the study area. This anomaly is linear, with a general NNW-SSE orientation, subparallel to the Kampti shear zone. The second Au anomaly, to the northwest, is more confined and sub-circular in appearance within sedimentary rocks. Manganese (Mn), copper (Cu), nickel (Ni) and zinc (Zn) anomalies overlap Au anomalies in mafic and intermediate volcanic formations. Molybdenum (Mo) shows rather diffuse signals of interest in the study area. In the central-eastern part of the study area, anomalies in lead (Pb) and strategic metals such as uranium, tantalum, and niobium (U, Ta-Nb) are defined and show sub-circular trends. Silver (Ag) is scattered throughout the study area. Cobalt (Co), titanium (Ti) and vanadium (V) anomalies are in the southeast of the study area and are well circumscribed, while lithium (Li) anomalies are scattered but predominate in the southwest and central east.

Table 3: Distribution of hydrothermal alteration minerals according to lithological units.

Alteration / Rock	Propylitic (carb-chl-ép-alb)	Phyllic (ser-mus)	Potassic (bio-k-felds)	Silica-carbonate	Greisen (qz-mus-carb-chl)	Tourmaline (qz-tz)
Basalt	++++	++	+	+++		
Volcanoclastic	++++	+++	+	+++		
Andesite	++++	+++	+++	+++		
Sediment	++++	++++	+++	+++		++
Gabbro	++++	++	+	+++		
Felsic bodies	++++	+++	++	+++	+++	+
Vein	++	+	+	++++		+
Gneiss	+	++++	+++	++++		+

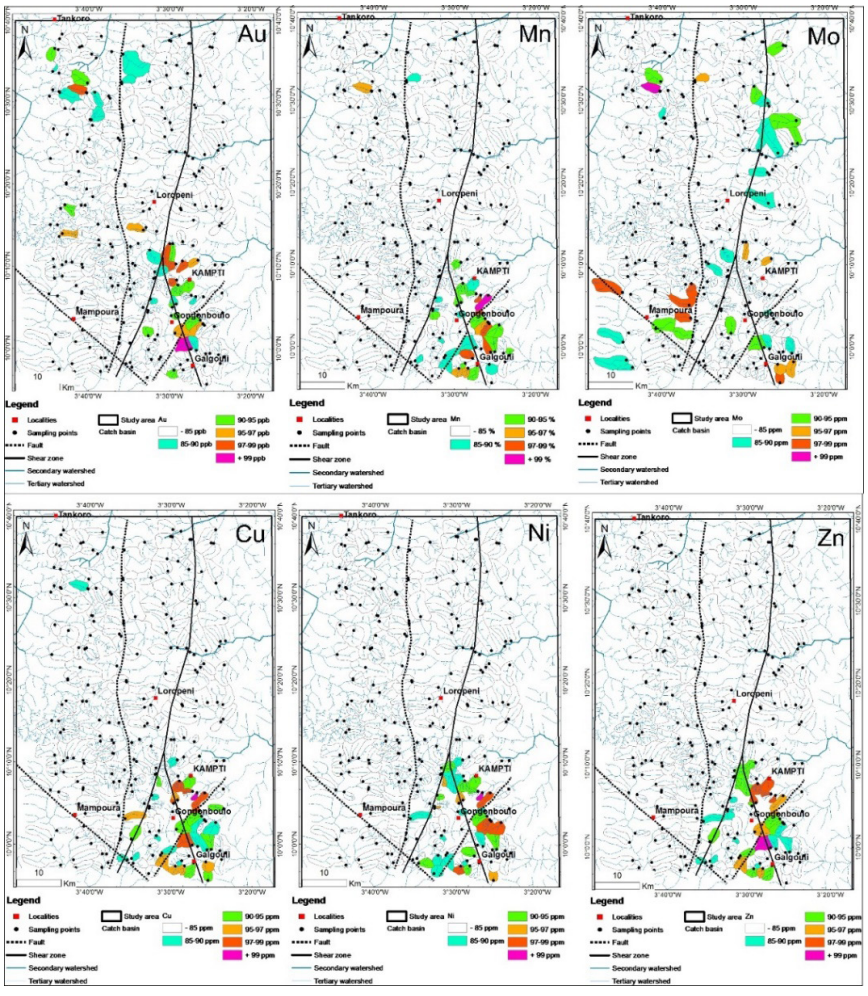

Figure 8: Spatial distribution of the metal anomalies from the stream sediment survey in this study.

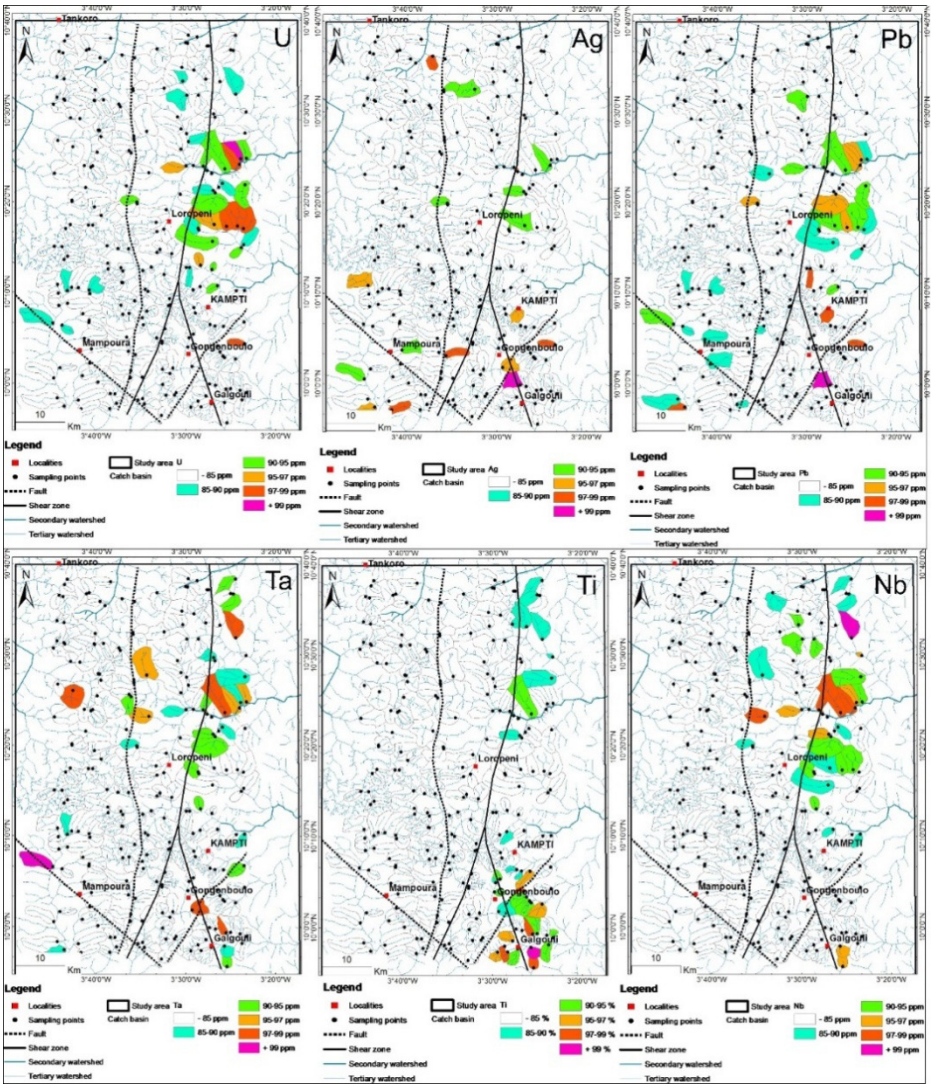

Figure 8 (continued)

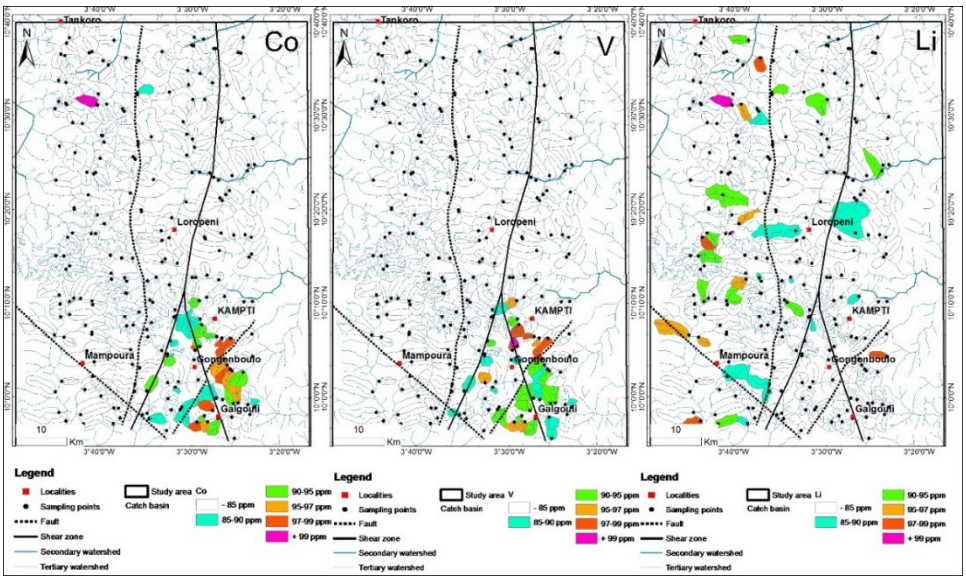

Figure 8 (continued)

Geological context of the metal signatures associations

Stream sediment-related geochemical anomalies are generally expressed over large areas; consequently, the delineation of anomalous zones for each metal remains debated. From the collected and interpreted data, four groups of metal associations are highlighted (Fig. 9): (i) the Kampti polymetallic anomaly, to the southeast, comprises several anomalies, notably in gold (Au), manganese (Mn), copper (Cu), nickel (Ni), zinc (Zn), cobalt (Co), titanium (Ti) and vanadium (V). These anomalies occur along the NNW Kampti fault, which extends from Galgouli over a strike length of 35 km and are associated with the mafic volcanics of the Kampti greenstone, (ii) the Loropeni polymetallic zone north of Kampti, grouped into two sub-zones of subcircular shape in the granitic pluton. This zone is characterized by the presence of U-Ta-Nb mineralization in the southern sub-zone and Ta-U in the northern sub-zone.Uranium (U), niobium (Nb) and tantalum (Ta) are generally associated with the granite plutons; (iii) the Tankoro Au-Mo anomaly in epiclastic sediments and shales that extends over 8 km x 3.5 km (Au values ranging from 44 to 133 ppb and Mo from 1.73 to 2.37 ppm); and (iv) Mampoura Au and Li-U occurrences around the felsic intrusion to the southwest of the study area.

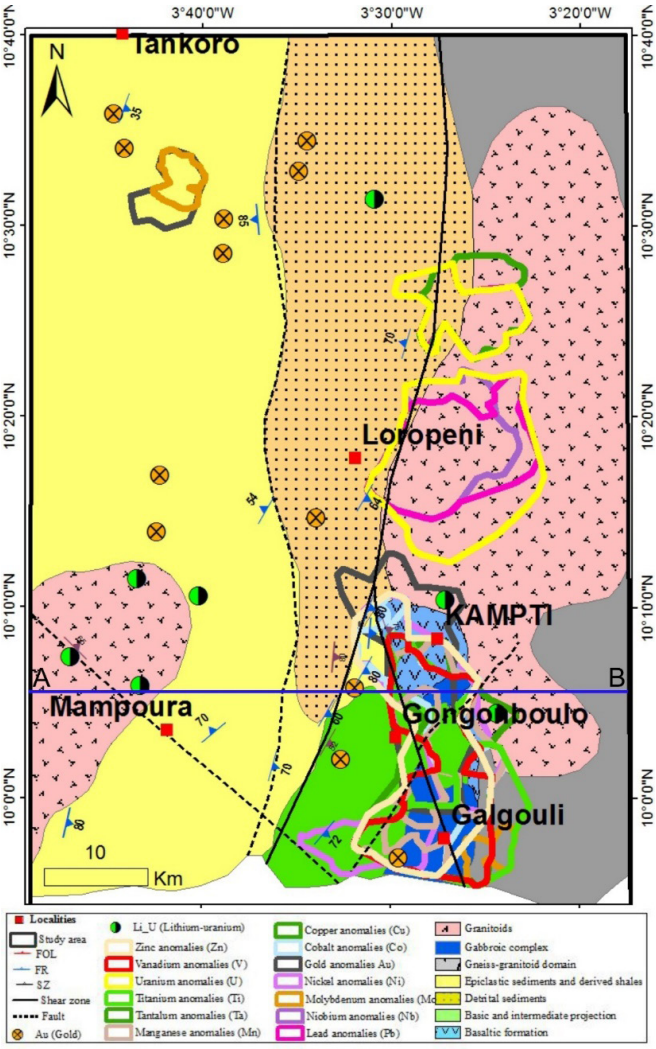

Figure 9**:** Metal anomalies and occurrences of Kampti-Loropeni greenstone.

DISCUSSION

Geology and metal distribution

Metal signatures defined through stream sediments geochemistry are distributed in both the intrabelt basin and the magmatic rocks (Fig. 9-10). Within the meta-sedimentary basin, the Au, Li-U and Au-Mo anomalies could have been derived from the the main and secondary faults that crossed the volcanogenic sediments and detrital sequence. A cluster of Li-U anomaly to southwest is in the granitoids intrusion. On the magmatic rocks, clusters of metal anomalies are observed in the both area: (i) U-Nb-Ta anomalism in the Loropeni area associated with granitoid batholith and at the contact fault between two lithological domains. (ii) V-Ti-Ni-Zn-Co-Au-Mn associated with the volcanic and mafic intrusions of the Kampti area. The anomalies are elongated NNW subparallel to the fault which crosses those lithological sequences.

Most of the U, Ta and Li anomalies identified in that study lies in granitoid domain where some pegmatite dykes where mapped. Several papers highlighted relationship between granite intrusions and strategic metal (Michaud 2019, Masurel *et al*. 2021). It has proven that rare metal granites show high enrichments in volatiles (F, Li, P, B) and in metals such as Li, Sn, Nb and Ta. In Burkina Faso, several strategic minerals occurrences were characterized associated to granitoids at Mangodara (Li-Nb) (Bonzi 2021) as well gold related porphyry granodiorite (Masurel *et al*. 2019, Ilboudo *et al*. 2018). Gold and base metal group (Cu-Zn-Ni, Au-Mn, Co, Ti-V) identified in the Kampti greenstone are both lithological and fault controls regarding the distribution of the anomalies. The concentration of those metals was described of VMS type in similar geological setting (Napon 1988, Ilboudo *et al*. 2013).The polymetallic association described here is well documented in other orogenic gold deposits of the West African craton (Milési *et al*. 1992, Bourges *et al*. 1998, Allibone *et al*. 2002).

Significance of anomalies and guide for exploration

Paleoproterozoic gold deposits in the West African Craton are not associated with any particular set of plutonic rocks (Goldfarb *et al*. 2017). Although granitoid-hosted gold deposits are known in the West African craton, the brittly deformed hosts considered as the key factor that controlled the formation of these deposits (Oberthür *et al*. 1998, Allibone *et al*. 2004). The Paleoproterozoic gold deposits at Bonikro Au-(Mo) (Masurel *et al*. 2019) and Morila (McFarlane *et al*. 2001) are examples of plutonism-associated mineralization. In northern Burkina Faso, a spatial relationship has been established between the Bélahourou granitic pluton and gold mineralization (Ilboudo *et al*. 2018, Sawadogo *et al*. 2018), as well in Ghana's Ashanti belt (Parra-Avilla *et al*. 2015).

Some base metals such as Cu, Ni and Zn, and the highly strategic metal such as Ta, Nb, U and Li were detected in the Kampti and Loropeni areas. These two commodity groups have various sources (magmatic, sedimentary, metamorphic, hydrothermal). In our context, the Nb-Ta-U geochemical anomalies described in the study area may reflect pegmatite- or sodic granite-type lithologies, as it is the case at Issia in Cote d'Ivoire (Allou *et al*. 2005). Li anomalies could be linked to highly differentiated leuco-granitic to pegmatitic acid magmatism (Michaud 2019, Bonzi 2022).

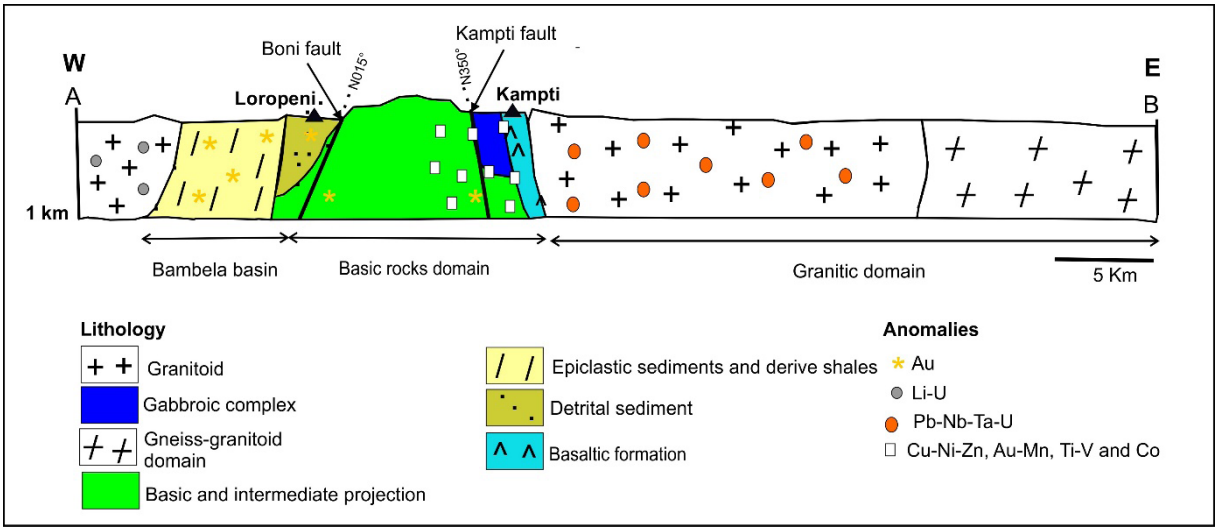

Figure 10: Geological cross section of the study area showing the relationship of anomalies to geology.

While previous studies carried out by the BUMIGEB have highlighted some targets such the polymetallic target of Kampti, the present study identifies the strategic metal target of Loropeni, Mampoura's Au and Li-U target.

Finally, detailed mapping coupled with multielement geochem studies of a tight soil grid,ground geophysics and drill targeting will enable to better highlight (i) the pegmatite dykes that contain the lithium host mineral spodumene, (ii) the uranium and thorium host mineral monazite within the favourable granite, and (iii) assess economic concentration for gold and base metals. A detailed study of the structural grain of that metallogenic domain is recommended to understand the controls and the geodynamic evolution of the belt is crucial for mineral exploration and the valuable resources assessment.

CONCLUSION

The greenstone rocks of the study area were strongly affected by the deformation resulting from the regional NW-SE compression. Several structures were developed including the regional S1 foliation and tight folding, mylonitic foliation and stretching along transpressive faults, crenulation, fractures, and veins. These deformations have induced intense circulation of hydrothermal fluids, as evidenced by the gold-bearing quartz veins subject to intense artisanal mining and the sluphidation (pyrite, chalcopyrite mainly) of the volcanic host rocks.

Studying the metal dispersion on wide area such Kampti-Loropeni using stream sediment geochemistry, the statistical percentile method applied to geochemical data combined with geophysical imagery and petrography, has detected groups of anomalies that could be of interest for prospecting. These are the Au-Mo, Cu-Ni-Zn, Ta-Nb-U and Li-U associations. These results partly confirm those of BUMIGEB, but also highlight the potential of the intrabelt basin particularly for gold and molybdenum, and Li-U in granite plutons which had not previously been highlighted. The polyphase nature of the magmatism, combined with a dynamic geological environment, would be conductive to the generation and circulation of fluids. Finally, the study shows that the Kampti and Loropeni greenstone along the Houndé beltare a reservoir of polymetallic resources that is still potential for exploration.

ACKNOWLEDGMENT

The authors would like to express their gratitude to the editor of «Bulletin de l'Institut Scientifique» ACHAB Mohammed and the anonymous reviewers for their significant contribution to the improvement of the manuscript.

REFERENCES

Allibone A., Teasdale J., Cameron G.*et al*. 2002. Timingand Structural Controls on Gold Mineralisation at the Bogoso Gold Mine, Ghana, West Africa. *Economic Geology*, 97, 949-969.

Allibone A., Hayden P., Cameron G. *et al*. 2004. Paleoproterozoic Gold Deposits Hosted by Albiteand Carbonate-Altered Tonalite in the Chirano District, Ghana, West Africa. *Economic Geology*, 99, 479-497.

Allou B.A., Lu H-Z., Guha. *et al*. 2005. Une corrélation génétique entre les roches Granitiques, et les Dépôts Eluvionnaires, Colluvionnaires Alluvionnaires de Columbo-Tantalite d'Issia, Centre-Ouest de la Côte D'Ivoire. *Exploration and Mining Geology*, 14 (1-4): 61-77.

Augustin J. & Gaboury D. 2016. Paleoproterozoic plume-related basaltic rocks in the Mana gold district in western Burkina Faso, west Africa: Implications for exploration and the source of gold in orogenic deposits. *Journal of African Earth Sciences*, 129, 17-30.

Augustin J., Gaboury D. & Crevier M. 2017. Structural and gold mineralizing evolution of the world-classorogenic Mana district, Burkina Faso: Multiple mineralizing events over 150 million years. *Ore Geology Reviews*, 32.

Baratoux L., Metelka V., Naba S. *et al*. 2011. Juvenile Paleoproterozoic crust evolution during the Eburnean orogeny (~2.2-2.0 Ga), western Burkina Faso. *Precambrian Research*, 184 (191), 18-45.

Bellehumeur C., Marcotte D. & Jébrak M. 1994. Multi-element relationships and spatial structures of regional geochemical data from stream sediments, southwestern Quebec, Canada. *Journal of Geochemical Exploration,51*(1), 11-35. https://doi.org/10.1016/0375-6742(94)90003-5

Bessoles B. 1977. Géologie de l'Afrique : Le craton ouest-africain. Mémoire, 88, 403 p.

Boher M., Abouchami W., Michard A. *et al.* 1992. Crustal Growth in the West Africaat 2.1 Ga. *Journal of Geophysical Research*, 97, 345-369.

Bonkoungou I. 1994. Le Tarkwaien du sillon de Houndé (Burkina Faso) : un ensemble volcano-détritique acide calco-alcalin à 2.15 Ga. Etude pétrologique, métamorphique et structurale. *Thèse Doctorat de 3ème cycle, Université de Nantes, France, 419 p.*

Bonzi W. M-E., Vanderhaeghe O., Lichtervelde M.V.*et al*. 2021. Petrogenetic links between metal-bearing pegmatites and TTG gneisses in the West African Craton : The Mangodara District of SW Burkina Faso.*Precambrian Research*, 364, 1-38.

Boulahcen A., Malo M., Labbé J-Y. *et al*. 2010. Nouvelles données géochimiques de sédiments de ruisseau dans le Centre-Nord de la Gaspésie (N° 09 ; p. 19). *Ministère de l'énergie et des réssources naturelles.*

Bourges F., Debat P., Tollon F. *et al*. 1998. The geology of the Tarpako gold deposit,Birimian greenstone belt, Burkina Faso, Afrique de l'Ouest. *Mineralium Deposita*, *33*, 591-605.

Castaing C., Billa M., Milési J-P. *et al.* 2003. *Notice explicative de la carte géologique et minière du Burkina Faso à 1/1000000, 3éme édition*. *Bureau de Recherches Géologiques et Minières (BRGM),* 148p.

Dan J.L., Katherine V.K., Roger M.K. *et al.* 2012. Geochemical mapping using stream sediments in west-central Nigeria: Implications for environmental studies and mineral exploration in West Africa. *Applied Geochemistry*, 7, 6, 1035-1052.

Goldfarb R. J., André-Mayer A.-S., Jowitt M. S. *et al*. 2017. West Africa : The World's Premier Paleoproterozoic Gold Province. *Economic Geology*, *112*, 123-143.

Hein A. A. K. 2015. The Bagassi gold deposits on the eastern margin of the Houndé greenstone belt, Burkina Faso. *Ore Geology Reviews*, 78, 660-666.

Ilboudo H., Sawadogo S., Naba S. *et al.* 2013. Structure et mode de mise en place dupluton granitique de Tiébélé (Burkina Faso) et son implication dans la concentration des anomalies en métaux de base (Zn-Pb-Cu) et en or (Au). *Bulletin de l'Institut Scientifique, section Sciences de la Terre*, *35*, 63-75.

Ilboudo H., Sawadogo S., Traoré A.S. *et al*. 2018. Intrusion-related gold, mineralization :Inata gold deposit, Bélahourou district, Northern Burkina Faso (West-Africa). *Journal of African Earth Sciences*, 52-58.

Khan J., Hua-Zhou Y., Kai-Xu C.*et al.* 2022. Geochemical prospecting of polymetalic mineralization in Gimbi-Nejo area, West Ethiopia. *Ore Geology Reviews*, 149.

Koffi Y. H., Wenmenga U. &Djro S. C. 2016. Tarkwaian Deposits of the Birimian Belt ofHoundé: Petrological, Structural and Geochemical Study (Burkina Faso, West Africa). *International Journal of Geosciences,*7, 685-700.

Lüdtke G., Hirdes W., Konan G. *et al*. 1998. Géologie de la région Haute Comoé Nord-Feuilles Kong (4b et 4d) et Téhini-Bouna (3a à 3d). *Direction de la géologie Abidjan Bulletin*, Abidjan.

Masurel Q., Thébaud N., Allibone A. *et al*. 2019. Intrusion-related affinity and orogenic gold overprint at the Paleoproterozoic Bonikro Au-(Mo) deposit (Côte d'Ivoire, West African Craton). *Mineralium Deposita*, 24.

Masurel Q., Eglinger A., Thébaud N. *et al.* 2021. Paleoproterozoic gold events in the southern West African Craton : review and synopsis. *Mineralium Deposita* 57, 513–537.

McFarlane R. M. C., Mavrogenes J., Lentz D. *et al*. 2001. Geology and Intrusion-Related Affinity of the Morila Gold Mine, Southeast Mali. *Economic Geology*, *106*(5), 727-750.

Michaud J. 2019. *Les granites à métaux rares : Origine, mise en place et mécanisme de la transition magmatique—Hydrothermale*. Thèse Doctorat de 3ème cycle, Université d'Orléans, France, 366 p.

Milési J. P., Ledru P., Feybesse J. L. *et al.* 1992. Early Proterozoic ore deposits and tectonics of the Birimian orogenic belt, West Africa. *Precambrian Research*, *58*, 305-344.

Nanema M., Wenmenga U. & Ilboudo H. 2017. Geochemical and Geodynamic Constrain of Tholeiitic Volcanism and Related Intrusions in The Kampti Gold District, Southwest Burkina Faso: Implication for Mineral Exploration. *Earth Science Research*, *7*(1), 76-93.

Nanema M. 2021. *Contraintes géologiques et facteurs de contrôle des gîtes polymétalliques de la ceinture Birimienne de Kampti, Burkina Faso-Afrique de l'Ouest*. Thèse Doctorat de 3ème cycle, Université Joseph KI-ZERBO, Ouagadougou, Burkina Faso, 234 p.

Napon S. 1988. *Gisement d'amas sulfuré (Zn-Ag) de Perkoa dans la province du Sangyé (Burkina Faso) : Cartographie, étude pétrographique, géochimique et métallogénique*. Thèse Doctorat de 3ème cycle, Université de FRANCHE-COMPTE, BESANCON, France, 302 p.

Oberthur T., Vetter U., Davis D. W.*et al*. 1998. Age constraints on gold mineralization and Paleoproterozoic crustal evolution in the Ashanti belt of southern Ghana. *Precambrian Research*, 89, 129-143.

Parra-Avila L. A., Bourassa Y., Miller J. *et al*. 2015. Age constraints of the Wassa and Benso mesothermal gold deposits, Ashanti Belt, Ghana, West Africa. *Journal of African Earth Sciences*, 11.

Pouclet A., Vidal M., Delor C. et al. 1996. Le volcanisme birimien du nord-est de la Côte D' Ivoire, mise en évidence de deux phases volcanotectoniques distinctes dans l'évolution géodynamique du Paléoprotérozoique. *Bulletin de la Société Géologique*, France 167, 529-541.

Sawadogo S., Naba S., Ilboudo H. *et al*. 2018. The Belahourou granite pluton (Djibo greenstone belt, Burkina Faso) : Emplacement mechanism and implication for goldmineralization along a shear zone. *Journal of African Earth Sciences*, 38p.

Trépanier S. 2006. Identification de domaines géochimiques à partir des levés régionaux de sédiment de fond delac - Phase 2. *Rapport de projet 2005-03*, 83 p.

Zuo R., Wang J., Xiong Y.*et al*. 2021. The processing methods of geochemical exploration data : past, present, and future. *Applied Geochemistry*, 9 p.

Manuscrit reçu le 22/06/2023
Version révisée acceptée le 13/06/2024
Version finale reçue le 08/07/2024
Mise en ligne le 09/07/2024